

1 Dengue virus hijacks a noncanonical oxidoreductase function of a cellular  
2 oligosaccharyltransferase complex

3

4 David L. Lin<sup>a</sup>, Natalia A. Cherepanova<sup>b</sup>, Leonia Bozzacco<sup>c</sup>, Margaret R. Macdonald<sup>c</sup>,  
5 Reid Gilmore<sup>b</sup>, and Andrew W. Tai<sup>a,d,e,\*</sup>

6

7 Department of Microbiology and Immunology, University of Michigan Medical School,  
8 Ann Arbor, Michigan, USA<sup>a</sup>; Department of Biochemistry and Molecular Pharmacology,  
9 University of Massachusetts Medical School, Worcester, Massachusetts, USA<sup>b</sup>;  
10 Laboratory of Virology and Infectious Disease, The Rockefeller University, New York,  
11 New York, USA<sup>c</sup>; Division of Gastroenterology, Department of Internal Medicine,  
12 University of Michigan Medical School, Ann Arbor, Michigan, USA<sup>d</sup>; Medicine Service,  
13 Ann Arbor Veterans Administration Health System, Ann Arbor, Michigan, USA<sup>e</sup>

14

15 **Running Head:** MAGT1 is required for DENV replication

16

17 \* Address correspondence to Andrew W. Tai, [andrewwt@umich.edu](mailto:andrewwt@umich.edu)

18

19 **Abstract word count: 221**

20 **Manuscript word count: 6,492**

21 **Abstract**

22           Dengue virus (DENV) is the most common arboviral infection globally, infecting  
23 an estimated 390 million people each year. We employed a genome-wide CRISPR  
24 screen to identify host dependency factors required for DENV propagation, and  
25 identified the oligosaccharyltransferase (OST) complex as an essential host factor for  
26 DENV infection. Mammalian cells express two OSTs containing either STT3A or STT3B.  
27 We found that the canonical catalytic function of the OSTs as  
28 oligosaccharyltransferases is not necessary for DENV infection, as cells expressing  
29 catalytically inactive STT3A or STT3B are able to support DENV propagation. However,  
30 the OST subunit MAGT1, which associates with STT3B, is also required for DENV  
31 propagation. MAGT1 expression requires STT3B, and a catalytically inactive STT3B  
32 also rescues MAGT1 expression, supporting the hypothesis that STT3B serves to  
33 stabilize MAGT1 in the context of DENV infection. We found that the oxidoreductase  
34 CxxC active site motif of MAGT1 was necessary for DENV propagation as cells  
35 expressing an AxxA MAGT1 mutant were unable to support DENV infection.  
36 Interestingly, cells expressing single-cysteine CxxA or AxxC mutants of MAGT1 were  
37 able to support DENV propagation. Utilizing the engineered peroxidase APEX2, we  
38 demonstrate the close proximity between MAGT1 and NS1 or NS4B during DENV  
39 infection. These results reveal that the oxidoreductase activity of the STT3B-containing  
40 OST is necessary for DENV infection, which may guide the development of antivirals  
41 targeting DENV.

42

43 **Importance**

44           The host oligosaccharyltransferase (OST) complexes have been identified as  
45 essential host factors for Dengue virus (DENV) replication; however, their functions  
46 during DENV infection are unclear. A previous study showed that the canonical OST  
47 activity was dispensable for DENV replication, suggesting that the OST complexes  
48 serve as scaffolds for DENV replication. However, our work demonstrates that one  
49 function of the OST complex during DENV infection is to provide oxidoreductase activity  
50 via the OST subunit MAGT1. We also show that MAGT1 associates with DENV NS1  
51 and NS4B during viral infection, suggesting that these non-structural proteins may be  
52 targets of MAGT1 oxidoreductase activity. These results provide insight to the cell  
53 biology of DENV infection, which may guide the development of antivirals against DENV.

54

## 55 **Introduction**

56           Dengue virus (DENV) is an enveloped positive-sense single-stranded RNA  
57 flavivirus that infects an estimated 390 million people each year, making it the most  
58 commonly acquired arbovirus infection (1). An effective vaccine that protects against all  
59 four DENV serotypes remains elusive, and to date there are no antivirals approved for  
60 the treatment of DENV infection (2).

61           DENV encodes a single open reading frame that is translated into a polyprotein,  
62 which is processed by both cellular and viral proteases at the endoplasmic reticulum  
63 (ER)(3). DENV, as an obligate intracellular parasite, is dependent on host-cell proteins  
64 to replicate its genome and produce progeny virus. The cellular factors involved in  
65 DENV replication have not been well described; however, two genome wide screens to

66 identify such DENV host dependency factors have recently been published, identifying  
67 the oligosaccharyltransferase (OST) complexes as essential to DENV replication (4, 5).

68 STT3A and STT3B, the catalytic components of the OST complexes, were  
69 identified as essential host factors for DENV replication in these screens. There are two  
70 distinct OST complexes in mammalian cells that incorporate either STT3A or STT3B as  
71 their catalytic subunit (6). Both STT3A and STT3B are oligosaccharyltransferases that  
72 catalyze the transfer of high mannose oligosaccharides onto target proteins in the  
73 lumen of the ER (6). STT3A and STT3B can glycosylate specific asparagine residues  
74 within the Asn-X-Ser/Thr sequon on target proteins. While STT3A is likely responsible  
75 for co-translational glycosylation of nascent proteins entering the ER lumen, STT3B is  
76 responsible for post-translational glycosylation of proteins with sequons skipped by  
77 STT3A (7).

78 Both of the OST complexes share several non-catalytic subunits—RPN1, RPN2,  
79 OST4, OST48, DAD1, and TMEM258 (6). MAGT1 and its paralog TUSC3 are specific  
80 subunits of the STT3B complex that are important for complete glycosylation of STT3B  
81 target proteins. MAGT1 and TUSC3 are thioredoxin homologs that harbor a conserved  
82 CxxC motif important for oxidoreductase activity (8, 9). MAGT1 and TUSC3, through  
83 their CxxC active sites, may form mixed disulfides with cysteines of a target protein,  
84 delaying native disulfide bond formation, and granting STT3B access to target sequons  
85 poorly accessible to STT3A. Loss of MAGT1 and TUSC3, or abrogation of the CxxC  
86 motif, leads to hypoglycosylation of STT3B specific substrates (8).

87 Marceau et al. demonstrated that DENV is dependent on both STT3A and  
88 STT3B, and that the oligosaccharyltransferase activity of each of these subunits is not

89 necessary for DENV replication (4). The authors proposed that the OST complexes act  
90 as scaffolds for DENV replication complexes to form. However, our data provide  
91 evidence that the STT3B-containing OST, through the MAGT1 subunit, provides a  
92 required catalytic activity for efficient DENV replication and not simply a scaffolding  
93 function.

94 In this work, a whole-genome CRISPR knockout screen was used to identify  
95 cellular factors required for DENV propagation. We confirm that both of the OST  
96 complexes are required for DENV replication, and that the oligosaccharyltransferase  
97 activities of either STT3A or STT3B OSTs are dispensable for DENV propagation.  
98 Importantly, however, knockout of STT3B leads to loss of MAGT1 expression, and loss  
99 of MAGT1 alone is sufficient to block DENV propagation. Additionally, the CxxC  
100 catalytic oxidoreductase active site of MAGT1 or TUSC3 is required for DENV  
101 propagation. Lastly, we find that DENV NS4B can be glycosylated by STT3B in a  
102 MAGT1-dependent manner, and that NS4B resides in close proximity to MAGT1 during  
103 DENV infection. Together, these data suggest that STT3B serves to stabilize MAGT1 in  
104 the context of DENV infection, and that the catalytic oxidoreductase activity of MAGT1  
105 is required for DENV propagation.

106

## 107 **Results**

### 108 **A whole genome CRISPR screen reveals that DENV is dependent on the** 109 **oligosaccharyltransferase complexes.**

110 We employed a CRISPR-Cas9 pooled screening approach to identify host  
111 proteins necessary for DENV-mediated cell death in Huh7.5.1 human hepatoma cells

112 (Fig. 1A). Among the top-ranked hits were multiple subunits of the host  
113 oligosaccharyltransferase (OST) complexes, including the two catalytic subunits *STT3A*  
114 and *STT3B*. Single-guide RNAs (sgRNAs) targeting genes encoding the two unique  
115 subunits of the *STT3A* and *STT3B* complexes, *DC2* and *MAGT1* respectively, were also  
116 significantly enriched in the screen. In addition, two shared OST subunits, *RPN2* and  
117 *OST4*, were significant hits. To validate three of the hits from the screen, we generated  
118 *STT3A*, *STT3B* and *MAGT1* knockout Huh7.5.1 cells through stable transduction of the  
119 pLENTICRISPRv2 construct encoding both the *S. pyogenes* Cas9 protein and an  
120 sgRNA. The knockouts were confirmed by Western blot. Importantly, in *STT3B*  
121 knockout cells, *MAGT1* protein is also depleted (Fig. 2A), as its stability requires  
122 interaction with *STT3B* (8). We then infected these cells with a luciferase reporter  
123 dengue virus (luc-DENV), where luciferase activity directly correlates with viral  
124 propagation. Three days post-infection, we assessed luciferase activity and saw a  
125 significant and marked decrease in luciferase activity in *STT3A*, *STT3B*, and *MAGT1*  
126 knockout cells compared to control cells transduced with a control GFP-targeting  
127 sgRNA, demonstrating that protection from DENV-mediated cell death in these  
128 knockout cells is mediated by inhibition of DENV infection rather than by a block of cell  
129 death signaling pathways. The viability and growth of *STT3A*, *STT3B*, or *MAGT1*  
130 knockout cells was similar to control cells (Fig. S1). These data validate the results from  
131 the screen and show that *STT3A*, *STT3B*, and *MAGT1* are all required for efficient  
132 DENV propagation.

133         Comparison of this screen's hits to two previously published whole-genome  
134 DENV screens, one using siRNA knockdown and another using a pooled CRISPR

135 knockout format (4, 5) (Table S1), revealed high overlap with the CRISPR screen by  
136 Marceau et al. Fifteen of the top 25 hits in our screen were identified in their screen  
137 (Table S1). The remarkable similarity between the two CRISPR screens demonstrates  
138 the technical reproducibility of pooled CRISPR screens for the identification of host  
139 dependency factors.

140

141 **The OSTs are required to support efficient infection by Zika virus but not other**  
142 **flaviviruses**

143 We next asked whether other arboviruses also depend on the same OST  
144 complexes, and used flow cytometry to determine whether infection was impaired in  
145 STT3A or STT3B knockout cells. We infected cells with DENV-2, Zika virus (ZIKV),  
146 West Nile virus, Yellow Fever virus, Sindbis virus, Venezuelan Equine Encephalitis virus,  
147 or Chikungunya virus and compared the percentage of infected cells in OST knockout  
148 cells compared to control. Consistent with our other results, we found that DENV-2  
149 infection was dramatically reduced in OST knockout cells compared to control (Fig. S2).  
150 We also found that ZIKV infection was moderately, but significantly, reduced in STT3A  
151 and STT3B knockout cells indicating that the OSTs may also play a role during ZIKV  
152 infection (Fig. S2). However, we did not find a significant decrease in the propagation of  
153 the other viruses tested.

154

155 **The catalytic oligosaccharyltransferase activity of the OST complexes is not**  
156 **required for DENV replication.**

157 In order to confirm the specificity of our knockout cell lines, sgRNA-resistant  
158 *STT3A*, *STT3B*, and *MAGT1* were then introduced by lentiviral transduction into the  
159 corresponding knockout cell lines to rescue *STT3A* (Fig. 2B) or *STT3B* (Fig. 2C)  
160 expression. Importantly, we found that exogenous expression of *STT3B* in *STT3B*  
161 knockout cells led to restoration of endogenous *MAGT1* expression (Fig. 2C).  
162 Exogenous expression of *STT3A* or *STT3B* rescued luc-DENV infection in *STT3A*-  
163 knockout or *STT3B*-knockout cells, respectively (Figs. 2B and C). These data confirm  
164 that *STT3A* and *STT3B* are specifically required for efficient DENV propagation.

165 Both *STT3A* and *STT3B* are oligosaccharyltransferases necessary for the  
166 transfer of glycans to asparagines on target substrates (7). Mutation of a conserved  
167 WWDYG motif to WAAYG inactivates oligosaccharyltransferase activity (10). *STT3A* or  
168 *STT3B* knockout cells expressing catalytically dead *STT3A* (*STT3A*-dead) or *STT3B*  
169 (*STT3B*-dead) were able to support similar levels of DENV infection as their wild-type  
170 counterparts, demonstrating that the catalytic activity of *STT3A* or *STT3B* is not required  
171 for DENV propagation (Figs. 2B and C).

172 We also confirmed that these constructs were indeed catalytically inactive by  
173 transfecting the rescued cells with plasmids to express either prosaposin (pSAP) or  
174 SHBG, specific N-glycosylation substrates of *STT3A* and *STT3B* respectively. By  
175 Western blot, a majority of pSAP remains hypoglycosylated, as evidenced by a more  
176 rapidly migrating band on SDS-PAGE from both *STT3A* knockout cells and *STT3A*-  
177 dead expressing cells (Fig. 2B). Similarly, a fraction of SHBG appears as a more rapidly  
178 migrating hypoglycosylated protein in both *STT3B* knockout cells and *STT3B*-dead  
179 expressing cells (Fig. 2C). These results demonstrate that glycosylation of *STT3A* and



180 STT3B specific endogenous substrates remains impaired in STT3A-dead and STT3B-  
181 dead expressing cells.

182 We also transfected a luciferase-DENV replicon into knockout cells to assess  
183 whether the specific step of viral replication requires STT3A or STT3B. We found that 3  
184 days post-transfection, there was a significant decrease in luciferase activity in *STT3A*  
185 and *STT3B* knockout cells compared to wild-type control (Fig. 2D). These data confirm  
186 that both of the OST complexes are required for DENV replication, consistent with  
187 previous data(4).

188 Together, these data suggest that STT3B stabilizes MAGT1 and that the  
189 canonical oligosaccharyltransferase activity of STT3B-containing OST complexes is not  
190 required for DENV propagation. These results support a model where STT3B is  
191 required to stabilize MAGT1, which in turn has its own specific function to support  
192 DENV replication. Therefore, we explored whether the catalytic activity of MAGT1 is  
193 required for DENV replication.

194

### 195 **The catalytic activities of TUSC3 or MAGT1 are necessary to support DENV** 196 **propagation**

197 Both MAGT1 and its paralog TUSC3 are thioredoxin homologs that harbor  
198 oxidoreductase activity through a conserved catalytic CxxC motif, and interact with  
199 STT3B but not STT3A (8). TUSC3 contains a peptide-binding pocket that may interact  
200 with proteins in a sequence specific manner (9). Cells lacking both MAGT1 and TUSC3  
201 are unable to fully glycosylate STT3B specific substrates (8). These data support a

202 model where MAGT1 or TUSC3 serve to form a mixed disulfide with a protein substrate,  
203 granting STT3B access to glycosylation sites that may otherwise be inaccessible.

204 In some cell types, TUSC3 expression is upregulated in the absence of MAGT1  
205 (8). Importantly, using both RT-PCR and Western blotting, we found that TUSC3 is not  
206 expressed in wild-type or *MAGT1* knockout Huh-7.5.1 cells, but is expressed in  
207 HEK293T cells (Fig 3A), consistent with previous reports (8). Therefore, we asked  
208 whether TUSC3 is capable of functionally replacing MAGT1 in the context of DENV  
209 infection. We found that *MAGT1* knockout Huh 7.5.1 cells transduced with a TUSC3-  
210 encoding lentiviral vector were able to support significantly increased DENV  
211 propagation compared to cells expressing neither MAGT1 nor TUSC3 (Fig. 3A). These  
212 data demonstrate that the expression of either MAGT1 or TUSC3 is required for DENV  
213 propagation, and that these two proteins are functionally redundant in the context of  
214 DENV propagation.

215 We next asked whether the enzymatic activity of MAGT1 or TUSC3 is required  
216 for DENV propagation. Expression of catalytically inactive AxxA mutants of MAGT1 or  
217 TUSC3 failed to rescue DENV propagation in MAGT1 knockout Huh7.5.1 cells (Fig. 3A  
218 and 3B), indicating that the oxidoreductase activity of MAGT1 or TUSC3 is required for  
219 DENV replication.

220 We also investigated whether MAGT1 knockout cells expressing single-cysteine  
221 active site MAGT1 mutants (CxxA and AxxC) are able to support DENV replication.  
222 Some single-cysteine mutants of ER resident oxidoreductases, such as protein disulfide  
223 isomerase (PDI), have been shown to retain oxidoreductase activity (11, 12).  
224 Interestingly, MAGT1 knockout cells expressing a single cysteine MAGT1 mutant were

225 able to support increased levels of DENV replication compared to knockout cells, albeit  
226 at levels lower than with wild-type MAGT1 rescue (Fig. 3B). This indicates that single  
227 cysteine MAGT1 mutants retain significant catalytic activity to support DENV infection.

228 All of these MAGT1 mutants were able to interact with STT3B using co-  
229 immunoprecipitation, thus demonstrating that MAGT1-AxxA's inability to support DENV  
230 replication is not due to a defect in STT3B association (Fig. S3). Together, these data  
231 demonstrate that the oxidoreductase activity of MAGT1 is required for DENV  
232 propagation, and that cells expressing single-cysteine MAGT1 are still able to support  
233 DENV replication.

234

### 235 **MAGT1 partially localizes to DENV replication compartments**

236 We next performed immunofluorescence microscopy on cells expressing an HA-  
237 tagged MAGT1 construct (MAGT1-HA) to visualize the localization of MAGT1 during  
238 DENV infection. In uninfected Huh-7 cells, both wild-type MAGT1 and MAGT1 mutants  
239 were distributed in an intracellular reticular pattern consistent with ER localization (Fig.  
240 3C). This supports the evidence that MAGT1 is an ER-localized component of the OST  
241 complex, rather than the proposal that MAGT1 contributes to magnesium import at the  
242 plasma membrane (8, 13). We also found that the distribution of the mutant MAGT1-  
243 AxxA was similar to that of wild-type MAGT1, demonstrating that the inability of cells  
244 expressing MAGT1-AxxA to support DENV replication is not due to defects in  
245 subcellular localization. DENV infection was associated with partial colocalization of  
246 MAGT1 with viral NS1 protein. These data are consistent with previous data showing

247 that the OST localized to sites of DENV induced vesicle packets and replication  
248 compartments(4).

249

### 250 **NS1 glycosylation is unchanged in STT3A, STT3B, and MAGT1 knockout cells**

251 We hypothesize that MAGT1 functions as an oxidoreductase, potentially affecting  
252 the folding of a DENV non-structural protein. We next asked which DENV proteins could  
253 be candidate substrates for MAGT1 oxidoreductase activity. All four DENV serotypes  
254 are impaired in their ability to propagate in *STT3B* knockout cells, which thus also lack  
255 MAGT1 expression (4). Therefore, we hypothesized that a viral target of MAGT1  
256 oxidoreductase activity must have cysteines in the ER lumen that are conserved across  
257 all four serotypes.

258 Four of the seven nonstructural proteins have cysteine residues predicted to be  
259 exposed to the ER lumen: NS1, NS2A, NS4A, and NS4B. Of these proteins, only NS1  
260 and NS4B have cysteines that are conserved across all four DENV serotypes. The  
261 DENV protein NS1 forms a dimer in the ER, is secreted as a soluble hexamer, and  
262 contains twelve cysteines, six disulfide bonds, and two N-glycosylation sites (14). The  
263 DENV protein NS4B contains three cysteines and two N-glycosylation sites (15).

264 We first investigated whether we could detect any changes in NS1 properties by  
265 immunoblotting of NS1 expressed in knockout and wild-type cells. We were unable to  
266 detect any changes in NS1 dimerization or glycosylation in *STT3A* or *STT3B* knockout  
267 cells (Fig. S4A). We also found that the pattern of NS1 glycosylation was unchanged  
268 after performing pulse-chase experiments in *STT3A*, *STT3B*, or *MAGT1/TUSC3*  
269 knockout cells (Fig. S4B). We were also unable to detect any interaction between NS1

270 and STT3B or MAGT1 by co-immunoprecipitation (not shown). In summary, these data  
271 suggest that glycosylation of NS1 is unaffected by the loss of STT3A, STT3B, or  
272 MAGT1, and that NS1 is not the target of MAGT1 oxidoreductase activity.

273

#### 274 **NS1-NS2A cleavage is unaffected by the loss of MAGT1**

275 We also explored the possibility that loss of MAGT1 could affect processing of  
276 NS1-NS2A by altering NS1 or NS2A folding. We were unable to find a defect in the  
277 processing of a NS1-NS2A-V5 expression construct, as NS2A migrated similarly in both  
278 wild-type and *STT3B* knockout cells (Fig. S5).

279

#### 280 **NS4B is an STT3B specific substrate**

281 We next determined whether we could find differences in NS4B exogenously  
282 expressed in OST subunit knockout cells by generating tagged constructs expressing  
283 C-terminally tagged DENV 2k-NS4B-HA (pNS4B-HA) or 2k-NS4B-V5 (pNS4B-V5).  
284 NS4B has been proposed to be glycosylated at two residues, N58 and N62 (15).  
285 Following transient expression of NS4B in Huh7.5.1 cells, we found three specific  
286 PNGase F sensitive bands that migrated at a higher molecular weight than  
287 unglycosylated NS4B, confirming that NS4B can be partially glycosylated under our  
288 experimental conditions (Fig. 4A).

289 NS4B glycosylation is impaired in *STT3B* or *MAGT1* knockout cells, and NS4B  
290 remains hypoglycosylated in 293T cells expressing catalytically inactive *STT3B* (Fig.  
291 4B). However, glycosylation of NS4B is not necessary for viral replication, because  
292 catalytically inactive *STT3B* rescues DENV replication in *STT3B* knockout cells.

293 Together, these data suggest that NS4B is an STT3B substrate that requires MAGT1 to  
294 be efficiently glycosylated, but NS4B glycosylation is not necessary for DENV infection.  
295 These data also provide evidence that NS4B directly interacts with MAGT1 and STT3B,  
296 therefore we performed assays to determine the nature of this interaction.

297

### 298 **Close proximity of MAGT to NS4B and NS1 during DENV infection**

299 Using conventional immunoprecipitation methods, we were unable to  
300 demonstrate a stable interaction between MAGT1 and NS4B. Therefore, we used the  
301 engineered peroxidase APEX2 to tag proteins in close proximity to MAGT1 during  
302 DENV infection. APEX2 catalyzes the biotinylation of proteins within a 5-10nm radius in  
303 the presence of biotin-phenol and hydrogen peroxide(16). We generated a construct in  
304 which APEX2 was inserted between the signal sequence and MAGT1, placing APEX2  
305 in the ER lumen near the MAGT1 active site. We stably transduced *MAGT1* knockout  
306 cells to express the APEX2-MAGT1 fusion protein, and induced APEX2-mediated  
307 biotinylation in DENV infected cells. After lysis of the cells, we performed affinity  
308 purification of biotinylated proteins using streptavidin beads followed by SDS-PAGE and  
309 immunoblotting.

310 We found that both NS1 and NS4B were specifically biotinylated by APEX2-  
311 MAGT1 in DENV infected cells (Fig. 5). To assess the specificity of APEX2 labeling, we  
312 probed for biotinylation of STT3A, which also associates with sites of DENV replication  
313 but does not interact with MAGT1 (4, 8), and found that STT3A is not biotinylated by  
314 APEX2-MAGT1 under these conditions (Fig. 5). Similarly, the integral ER membrane  
315 protein VAPA is not biotinylated by APEX2-MAGT1. On the other hand, EMC3, another

316 ER protein necessary for flavivirus propagation that was a hit in our screen and interacts  
317 with the OST complex (5), was biotinylated. These data are consistent with the model  
318 that MAGT1 likely resides at sites of DENV replication and either associates with or is in  
319 close physical proximity to DENV non-structural proteins.

320

### 321 **The redox status of NS4B is unchanged in the absence of MAGT1**

322 We hypothesized that NS4B disulfide bond arrangement is mediated by MAGT1.  
323 To test this, we used Western blots to examine changes in migration of NS4B after  
324 treating cell lysates with maleimide-PEG (mPEG), which covalently bonds to reduced  
325 thiols present on free cysteine residues that do not participate in disulfide bonds. The  
326 mPEG reagent has an average molecular weight of 5 kDa, resulting in a shift in the  
327 apparent molecular weight of modified proteins visualized by Western blot. We used  
328 mPEG to probe the redox state of cysteines present in NS4B. DENV NS4B has three  
329 conserved cysteines that may participate in disulfide bonds. As a negative control, we  
330 lysed cells in the presence of N-ethylmaleimide (NEM), which covalently binds to and  
331 blocks all reduced cysteines, rendering them mPEG-nonreactive (Fig. S6, lanes 1 and  
332 2). As a positive control, we treated lysates with Tris(2-carboxyethyl)phosphine  
333 hydrochloride (TCEP), which reduces all cysteines, allowing subsequent mPEG  
334 modification of all cysteines (Fig. S6, lane 5).

335 mPEG modified NS4B, when expressed in isolation, migrates the same in both  
336 wild-type and *STT3B* knockout cells, indicating that MAGT1 does not affect the cysteine  
337 redox state of NS4B (Fig. S6, lanes 3 and 4). Additionally, a fraction of mPEG-modified  
338 NS4B (lanes 3 and 4) runs at the same apparent molecular weight as fully reduced

339 TCEP-treated NS4B treated with mPEG (lane 5), indicating that at steady state, a  
340 fraction of NS4B molecules contains fully-reduced cysteines. However, another fraction  
341 of NS4B is modified by fewer mPEG molecules (lanes 3 and 4), demonstrating that  
342 some NS4B molecules may contain oxidized cysteines in the form of intra- or  
343 intermolecular disulfide bonds.

344 While our results indicate that MAGT1 does not modulate NS4B cysteine redox  
345 state when expressed in isolation, they do not rule out the possibility that MAGT1  
346 modulates NS4B cysteine redox status transiently and/or in the context of authentic viral  
347 infection. Further experiments will have to be carried out to determine whether NS4B  
348 disulfide bonds exist during infection.

349

## 350 **Discussion**

351 Our results demonstrate the high reproducibility of whole genome CRISPR  
352 screens compared to the low overlap among hits from siRNA-based screens for host  
353 cofactors of viral infection. We compared the top hits from our CRISPR screen to those  
354 recently published and found that 15 of the top 25 hits from our screen were in the top  
355 1% of the other's (4). In contrast, three independent siRNA screens for host  
356 dependency factors of DENV infection performed by the same group identified over 150  
357 high confidence hits; however, only 14% of hits from one independent siRNA library  
358 overlapped with hits from another siRNA library, even when performed by the same  
359 investigators using the same infection conditions (5). This is consistent with meta-  
360 analyses demonstrating the low reproducibility of siRNA screens for viral host factors  
361 (17).



362           While there is a high degree of overlap between CRISPR screens for DENV, the  
363 number of significant hits is relatively low compared to those obtained from RNAi  
364 screens. For example, the pooled results of the three siRNA screens for DENV yielded  
365 hundreds of hits whereas our CRISPR screen yielded fewer than 50 significant hits.  
366 This may be due in part to some DENV host factors also being necessary for cellular  
367 survival or growth. Additionally, using cell survival from lethal viral challenge as a  
368 readout is highly stringent and will increase the false-negative rate, as only partial  
369 suppression of DENV infection may not be sufficient to protect cells from death. Thus,  
370 experimental readouts that can capture intermediate phenotypes are likely to reveal  
371 additional host dependency factors for DENV infection.

372           The events at the endoplasmic reticulum that direct the formation of a functional  
373 dengue virus replication organelle remain incompletely understood. In this study, a  
374 whole-genome CRISPR screen reveals a non-canonical function of the OST complex  
375 that serves to support DENV infection. STT3B, the subunit of the OST complex that  
376 provides oligosaccharyltransferase activity, is required to stabilize MAGT1 to support  
377 DENV replication. We show that MAGT1, or its homolog TUSC3, provides a catalytic  
378 oxidoreductase activity necessary for DENV to replicate.

379           On the other hand, we find that the N-glycosylation activity of STT3A or STT3B is  
380 dispensable for DENV propagation, in agreement with previous findings by Marceau et  
381 al. (4). Based on this observation, these authors suggested that the OST complexes  
382 serve as structural scaffolds for DENV to replicate. However, it is unclear why both  
383 STT3A- and STT3B-containing OST complexes would be required to serve a  
384 scaffolding function for DENV replication. Our data show that STT3B-containing

385 complexes serve more than a structural scaffolding function to support DENV replication,  
386 and in fact contribute a direct catalytic activity for DENV replication: namely, the  
387 oxidoreductase activity of MAGT1. We propose that the dependency of DENV  
388 replication on STT3B without requiring its oligosaccharyltransferase activity is explained  
389 by the loss of MAGT1 expression in the absence of STT3B.

390 Analogous to the dependence of MAGT1 on STT3B for stable expression, some  
391 subunits of the STT3A complex require STT3A for stable expression (18). We propose  
392 that there may be a specific function granted by the STT3A complex subunits  
393 DC2/OSTC or KCP2 that is necessary for DENV replication. In support of this  
394 hypothesis, DC2 was a hit in both CRISPR screens(4). However, the precise cellular  
395 function of DC2 is unknown.

396 We have shown that the CxxC catalytic motif of MAGT1 or TUSC3 is required for  
397 DENV propagation, and that TUSC3 can functionally replace MAGT1 in the context of  
398 DENV infection. Some cell types, including HEK293 cells, express both TUSC3 and  
399 MAGT1, while others, including hepatocytes and Huh7.5.1 hepatoma cells, express only  
400 MAGT1 (13). Importantly, TUSC3 expression is upregulated in HEK293 cells when  
401 *MAGT1* is knocked out (19). Thus, essential but functionally redundant functions of  
402 MAGT1 and TUSC3 in DENV replication will not be revealed in cell types capable of  
403 expressing both proteins.

404 Typically, both cysteines in the CxxC active site motif of an oxidoreductase are  
405 involved in catalyzing disulfide bond formation in a target protein. However, cells  
406 expressing CxxA or AxxC active site mutants of MAGT1 can support DENV propagation.  
407 Single-cysteine active site mutants of protein disulfide isomerase (PDI) have been

408 shown to retain partial reductase activity *in vitro*, and are still able to shuffle disulfide  
409 bonds and mediate native protein folding (11, 12). As depicted in Fig. S7, a single-  
410 cysteine reductase can act as a disulfide isomerase by attacking a non-native disulfide  
411 bond on a target protein, generating a mixed disulfide between the reductase (here  
412 MAGT1) and its target. An alternate cysteine from the target protein then resolves the  
413 mixed disulfide, forming the native disulfide bond and releasing the target protein from  
414 MAGT1. Previous studies have shown that a single-cysteine MAGT1 mutant exhibits  
415 partial catalytic activity when assessing glycosylation of an STT3B substrate (8). Single-  
416 cysteine MAGT1 could therefore serve as a disulfide isomerase in the context of DENV  
417 infection. Alternatively, single-cysteine MAGT1 may function in tandem with another ER-  
418 resident oxidoreductase to resolve the mixed disulfide, and generate a correctly folded  
419 target substrate.

420         However, this model is not easily reconciled with the observation that either  
421 single-cysteine or wild-type MAGT1 is capable of supporting DENV replication, because  
422 the majority of wild-type MAGT1 appears to be oxidized in cells, without reduced  
423 cysteines to attack disulfide bonds(8). One possibility is that a minor fraction of reduced  
424 MAGT1 or TUSC3 is sufficient to support DENV replication.

425         If MAGT1 does not directly catalyze disulfide bond rearrangement in a DENV  
426 protein such as NS4B, another possibility is that MAGT1, though its oxidoreductase  
427 activity, recruits a DENV protein to another cellular protein or complex. For example, the  
428 OST complex has recently been identified to associate with proteins in the ER  
429 membrane complex (EMC), which has been reported to act as a chaperone for  
430 multipass transmembrane proteins, of which NS4B is an example (20, 21). In this model,

431 MAGT1, through its oxidoreductase activity, might transiently interact with NS4B,  
432 recruiting it to the EMC as an NS4B chaperone. Our data showing that MAGT1 and  
433 EMC3 are in close proximity support this possibility. Further experiments need to be  
434 carried out to determine the exact mechanism by which MAGT1 supports DENV  
435 replication.

436 We carried out several experiments directed at the hypothesis that viral NS1  
437 and/or NS4B is a substrate of MAGT1, as these viral proteins harbor multiple cysteines  
438 conserved across all DENV serotypes that are also predicted to be accessible to  
439 MAGT1. We were unable to find any differences in NS1 dimerization or glycosylation in  
440 MAGT1 knockout cells compared to wild-type, suggesting that NS1 is correctly folded  
441 and processed in the absence of MAGT1.

442 However, we did find that NS4B can be glycosylated in an STT3B and MAGT1-  
443 dependent manner, lending support to the hypothesis that MAGT1 interacts transiently  
444 with NS4B. We probed the disulfide status of NS4B expressed in isolation, and found no  
445 apparent differences in NS4B cysteine accessibility to mPEG modification in the  
446 absence or presence of MAGT1 activity. We cannot exclude that MAGT1 is required for  
447 the correct folding of NS4B as we lack a suitable assay, nor can we exclude the  
448 possibility that MAGT1 is required for the correct folding or activity of a cellular protein  
449 necessary for DENV propagation.

450 Using co-immunoprecipitation methods, we were unable to demonstrate a stable  
451 interaction between MAGT1 and DENV non-structural proteins, likely due to the  
452 transient association between oxidoreductases and their target substrates(22). APEX2  
453 biotinylates targets within a < 20 nm radius, and has been used to demonstrate protein-

454 protein interaction (23). APEX2-MAGT1 induced biotinylation of both NS4B and NS1 in  
455 DENV infected cells, indicating that MAGT1 interacts with, or is at least in close  
456 proximity to, components of the DENV replication organelle in the ER. Of note, the  
457 APEX2-MAGT1 fusion protein did not biotinylate STT3A, which is also present in the ER  
458 membrane at DENV replication sites, demonstrating the specific APEX2 mediated  
459 biotinylation of proteins closely associated with MAGT1.

460 We also found that ZIKV infection is significantly reduced in STT3A or STT3B  
461 knockout cells, suggesting that ZIKV may also require the OST complex for efficient  
462 infection or replication. However, the other flaviviruses tested did not appear to be  
463 dependent on OST complex function, despite the common dependence of most  
464 flaviviruses on the host cell ER for replication organelle formation. Interestingly, the  
465 NS4B cysteines are not conserved among flaviviruses despite being conserved across  
466 all DENV serotypes.

467 In conclusion, our data demonstrate that the STT3B-containing OST complex  
468 serves a catalytic and non-canonical function during DENV replication, and not merely a  
469 scaffolding function. We hypothesize that this non-canonical oxidoreductase activity of  
470 MAGT1 acts on a DENV non-structural protein, such as NS4B, to mediate folding or  
471 recruitment of non-structural proteins to specific sites in the ER. Our results improve our  
472 understanding the cell biology of DENV infection, and also may potentially grant insight  
473 to the development of DENV antivirals that target MAGT1.

474

## 475 **Materials and Methods**

### 476 **Pooled CRISPR screen**

477 The Human GeCKOv2 plasmid library was a gift from Feng Zhang, acquired from  
478 AddGene. VSV-G pseudotyped GeCKOv2 lentiviruses were generated at the University  
479 of Michigan vector core. In brief, 16 million Huh-7 cells were transduced with the  
480 GeCKOv2 A or B lentiviral half-library at an MOI = 0.3 in 10 cm dishes. Cells were  
481 selected for 6 d post-transduction with 2 µg/mL puromycin, then infected with DENV-2  
482 16681 at an MOI = 0.1 for 2 weeks. Genomic DNA from surviving cells was harvested  
483 using a Quick-gDNA Midi kit (Zymo Research, Irvine, CA). The integrated sgRNAs were  
484 amplified using PCR, and Illumina adapters and barcodes were subsequently added by  
485 PCR as previously described (24). Sequencing was performed at the University of  
486 Michigan sequencing core on a MiSeq (Illumina, San Diego, CA), and data was  
487 analyzed using MaGeCK (25).

488

#### 489 **Plasmids and lentiviral transduction**

490 Individual sgRNAs targeting *STT3A*, *STT3B*, and *MAGT1* were generated in  
491 pLENTICRISPRv2 as previously described using the crRNA sequences listed in Table  
492 S2. The lentiCRISPR - EGFP sgRNA 1 was a gift from Feng Zhang (Addgene plasmid #  
493 51760).

494 The cDNA clone for *STT3A* was purchased from OriGene (RC201991; Rockville,  
495 MD). The cDNA clones for *STT3B* and *MAGT1* were described previously (19). The  
496 *TUSC3* gene was cloned by PCR from 293T cDNA. The sgRNA-resistant *STT3A*,  
497 *STT3B*, and *MAGT1* constructs were made using overlap extension PCR to introduce  
498 silent mutations either modifying the CRISPR protospacer adjacent motif or sgRNA  
499 basepair complementarity. The catalytically inactive *STT3B*, *STT3B*, *MAGT1*, and

500 *TUSC3* were generated using overlap extension PCR. These constructs were cloned  
501 into the lentiviral expression vector pSMPUW (Cell Biolabs, San Diego, CA). The  
502 constructs for expression of pSAP and SHBG have been previously described (26, 27).  
503 The pNS1-flag, pNS1-NS2A-V5, and pNS4B-HA constructs were generated by PCR  
504 using pD2/IC-30P-NBX as a template (28). Detailed descriptions of construction of  
505 these plasmids are available upon request.

506 Lentiviral expression constructs were used to generate VSV-G pseudotyped  
507 lentiviruses and for stable transduction of target cells as described in (29). Knockouts  
508 and expression were confirmed by Western blot.

509

## 510 **Viruses**

511 The infectious cDNA clone pD2/IC-30P-NBX encoding Dengue virus serotype 2  
512 strain 16681 was used to generate full-length viral RNA, and for construction of a  
513 reporter virus and replicon (28). In brief, the luciferase reporter virus luc-DENV was  
514 generated by overlap extension PCR, by fusion of a Renilla luciferase (Rluc) with C-  
515 terminal self-cleaving 2A peptide to the DENV capsid in a pD2/IC-30P-NBX  
516 background. The luciferase reporter replicon was generated as previously  
517 described(30). To generate wild-type DENV-2 virus, the pD2/IC-30P-NBX plasmid was  
518 linearized with XbaI (New England Biolabs, Ipswich, MA), in vitro transcribed, and  
519 capped with the m<sup>7</sup>G(5')ppp(5')A cap analog (New England Biolabs) using T7  
520 Megascript (Thermo Fisher Scientific, Waltham, MA). This RNA was transfected into  
521 Vero cells using TransIT mRNA reagent (Mirus Bio, Madison, WI). One week post-  
522 transfection, supernatant from transfected cells was 0.45 µm filtered and buffered with

523 20 mM HEPES. Cells were infected by replacing media on the cells with viral  
524 supernatant for 4 hr at 37C and 5% CO<sub>2</sub>. Afterwards, unbound virus was aspirated and  
525 replaced with fresh media. For luciferase reporter assays, cells were infected with the  
526 luciferase reporter virus luc-DENV at an MOI = 0.1 for 2 or 3 d and luciferase activity  
527 was measured with the Renilla Luciferase Assay System (Promega, Madison, WI) and a  
528 Synergy 2 plate reader (BioTek, Winooski, VT).

529 The recombinant infectious viruses used were as follows:

530 SINV-GFP, generated from pTE/5'2J/GFP (31), YFV-Venus, generated from pYF17D-  
531 5'C25Venus2AUbi (32), WNV-GFP, generated from pBELO-WNV-GFP-RZ ic (33),  
532 CHIKV-GFP generated from pCHIKV-LR 5'GFP (34), VEEV-GFP, a TC83 vaccine strain  
533 derivative generated from pVEEV/GFP (35), and DENV2-GFP a 16681 strain derivative  
534 generated from pDENV2-ICP30P-A-EGFP-P2AUb (36). Viral stocks were generated by  
535 electroporation of in vitro-transcribed RNA into WHO Vero cells (for DENV2-GFP) and  
536 BHK-21 cells (for SINV, YFV, WNV, CHIKV and VEEV). Zika virus (ZIKV), 2015 Puerto  
537 Rican PRVABC59 strain (37), was obtained from the CDC and passaged twice in Huh-  
538 7.5 cells.

539 Multiplicity of infection (MOI) was based on titers obtained on BHK-J cells for  
540 SINV, WNV, YFV and VEEV infections, and on Huh-7.5 cells for ZIKV. Titers were not  
541 available for YFV, CHIKV and DENV2, therefore different dilutions of viral stocks were  
542 tested.

543 Cells were seeded in a 24-well plate at  $5 \times 10^4$  cells/well for ZIKV or at  $1 \times 10^5$   
544 cells/well for other viruses. The next day, cells were infected for 90 min at 37°C in 2%  
545 FBS/PBS using a MOI of 1 for SINV, 0.01 and 0.001 for WNV and 0.8 for VEEV. We



546 used a 1:4 dilution for YFV, 1:10000 for CHIKV and 1:5 for DENV-2. Virus inoculum was  
547 removed, fresh complete media was added to the cells, and infections allowed to  
548 proceed for 10 h for SINV and VEEV, 24 h for CHIKV, 33 h for YFV, 48 h and 72 h for  
549 WNV, 58 h for DENV-2 and 48 h and 96 h for ZIKV. Experiments with WNV and CHIKV  
550 were carried out under biosafety level 3 containment. Infected cells were detached  
551 using Accumax Cell Aggregate Dissociation Medium (eBiosciences). Cells were  
552 pelleted, fixed in 2% paraformaldehyde and permeabilized using Cytotfix/Cytoperm (BD  
553 Biosciences). For ZIKV infected cells, E protein expression was detected with the 4G2  
554 monoclonal antibody (1:500 dilution), followed by incubation with Alexa Fluor 488-  
555 conjugated anti-mouse IgG antibody (Invitrogen) at 1:1,000 dilution. All samples were  
556 resuspended in 2% FBS/PBS. Fluorescence was monitored by FACS using an LSRII  
557 flow cytometer (BD Biosciences). Data were analyzed with FlowJo Software.

558

## 559 **Antibodies**

560 Western blots were performed using antibodies against STT3A (12034-1-AP), STT3B  
561 (15323-1-AP), MAGT1 (17430-1-AP), and proSaposin (10801-1-AP) from the  
562 Proteintech Group (Rosemont, IL). Antibodies against TUSC3 (SAB4503183) and Actin  
563 (A5316) were purchased from Sigma Aldrich (St. Louis, MO). The antibody against  
564 EMC3 (sc-365903) was purchased from Santa Cruz Biotechnology (Dallas, TX). The  
565 antibody against SHBG (MAB2656) was purchased from R&D systems (Minneapolis,  
566 MN). The antibody against HA (C29F4) was acquired from Cell Signaling (Danvers, MA).  
567 The anti-V5 antibody (R960-25) was purchased from Thermo Fisher Scientific. The anti-

568 NS1 monoclonal antibody 1F11 was a gift from the Dr. Malasit at the National Center for  
569 Genetic Engineering and Biotechnology in Thailand.

570

### 571 **Western blotting**

572 Cells were lysed in a buffer containing 20mM Tris pH 7.5, 100mM NaCl, 1% NP-40,  
573 10% glycerol, and 1mM EDTA with the addition of Halt protease inhibitor (Thermo  
574 Fisher). Lysates were cleared by centrifugation at 10,000 rpm for 10 minutes at 4C. LDS  
575 sample buffer was added and lysates were resolved by SDS-PAGE on 4-12% Bis-Tris  
576 NuPAGE Novex gels. Proteins were transferred to PVDF membranes, which were then  
577 blocked for 30 min in 5% nonfat dry milk in TBST. Antibodies were added at the  
578 following dilutions: STT3A (1:1000), STT3B (1:500), MAGT1 (1:1000), TUSC3 (1:1000),  
579  $\beta$ -actin (1:20000), HA (1:1000), V5 (1:5000), NS1 (1: 100). Membranes were incubated  
580 in primary antibody overnight at 4°C, then subsequently washed 3x with TBST for 15  
581 min each. Membranes were then incubated in blocking buffer with 1:500 of secondary  
582 HRP conjugated antibodies (ThermoFisher) for 1 h at room temperature. Blots were  
583 then washed and proteins were detected by the addition of SuperSignal West Femto  
584 substrate and immediate visualization on a LI-COR (Lincoln, Nebraska) imager or by X-  
585 ray film.

586

### 587 **APEX labeling and immunoprecipitation**

588 The APEX2-MAGT1 fusion construct was generated by overlap extension PCR.  
589 APEX2-mediated biotinylation and enrichment of biotinylated proteins was performed as  
590 previously described (38). A modification to the protocol was the addition of 20 mM N-

591 ethylmaleimide (NEM; Sigma Aldrich) to the lysis buffer to preserve native disulfide  
592 bonds. 10% of the lysates were reserved to be run as input controls. 1 µg of either V5 or  
593 HA antibody was added to immunoprecipitate respectively tagged proteins. Mixtures  
594 were rotated for 2 h at 4°C. 5 µl of Dynabeads protein G (ThermoFisher) were added to  
595 each tube and rotated for 1 h at 4°C. Complexes were washed 3x in 1x PBS with 0.1%  
596 Triton X-100. Proteins were eluted in 1x LDS sample buffer with 50mM Tris(2-  
597 carboxyethyl)phosphine hydrochloride (TCEP, Sigma Aldrich). Lysates were then  
598 subjected to SDS-PAGE and Western blotting as described above.

599

#### 600 **Pulse-chase analysis of NS1 glycosylation**

601 HEK293 cells were grown to 60% confluency in 60 mm dishes and transfected with 6 µg  
602 of NS1-FLAG expression plasmids using Lipofectamine 2000 (ThermoFisher) in Opti-  
603 MEM (ThermoFisher) according to the manufacturer's instruction. After 24 h, NS1  
604 substrates were labeled with Tran<sup>35</sup>S label (Perkin Elmer, Waltham, MA) by incubation  
605 in methionine- and cysteine free media containing 10% dialyzed FBS for 20 min before  
606 the addition of 200 µCi/mL of Tran<sup>35</sup>S label. Cells were labeled for 5 min, then 3.7 mM  
607 unlabeled methionine and 0.75 mM unlabeled cysteine were added and cells were  
608 incubated for an additional 20 min. Cells were lysed at 4°C by a 30 min incubation with  
609 1 mL of RIPA lysis buffer. Lysates were clarified by centrifugation (2 min at 13,000 rpm)  
610 and precleared by incubation for 2 h with rabbit IgG and a mixture of protein A/G  
611 Sepharose beads (Santa Cruz Biotechnology) before an overnight incubation with anti-  
612 FLAG antibody (Sigma Aldrich). Immunoprecipitates were collected with protein A/G-  
613 Sepharose beads then washed five times with RIPA lysis buffer and twice with 10 mM

614 Tris-HCl, pH 7.5 before eluting proteins with gel loading buffer. Where indicated,  
615 immunoprecipitated proteins were digested with Endoglycosidase H (New England  
616 Biolabs). Dry gels were exposed to a phosphor screen (Fujifilm, Valhalla, NY), and  
617 scanned with a Typhoon FLA9000 laser scanner (GE Healthcare, Chicago, IL).

618

### 619 **PNGase F digestion and maleimide-PEG assays**

620 Lysates were subjected to PNGase F (New England Biolabs) digestion as suggested by  
621 the manufacturer guidelines. Methoxypolyethylene glycol maleimide 5000 (mPEG;  
622 Sigma Aldrich) was dissolved in water to a 100 mM stock immediately prior to use. Cells  
623 were lysed in lysis buffer with the addition of either 20 mM NEM, 5 mM mPEG, or 0.5  
624 mM TCEP. Lysates were incubated at room temperature for 30 min prior to clearing by  
625 centrifugation at 10,000 rpm for 10 min. Supernatants with TCEP added were then  
626 supplemented with 5 mM mPEG to modify the now reduced cysteines. Lysates were  
627 resolved by SDS-PAGE and visualized by Western blot as described above.

628

### 629 **Immunofluorescence**

630 Huh 7.5.1 cells were plated on poly-D-lysine coated coverslips and infected with DENV-  
631 2 at an MOI = 0.1 or mock infected. Two days post-infection, cells were fixed in ice cold  
632 methanol for 1 h at -20C. Immunostaining with anti-HA (1:200) and anti-NS1 (1:50)  
633 antibodies was performed as described previously(39).

634

### 635 **Funding Information**

636 This work was supported by National Institutes of Health grants R01DK097374 (AWT),  
637 the Molecular Mechanisms of Microbial Pathogenesis Training Program 5T32AI007528  
638 (DLL), R01AI124690 (MRM) and R01GM043768 (RG). Microscopy was performed at  
639 the University of Michigan Microscopy & Image Analysis Laboratory with support from  
640 the University of Michigan Center for Gastrointestinal Research (National Institutes of  
641 Health P30DK034933). The funders had no role in study design, data collection and  
642 interpretation, or the decision to submit the work for publication.

643

#### 644 **Acknowledgments**

645 We thank Claire Huang (CDC) for providing the pD2/IC-30-P-NBX DENV cDNA clone,  
646 and Dr. Chunya Puttikhunt (Mahidol University, Thailand) for providing the NS1  
647 monoclonal antibody.

648

#### 649 **References**

650

- 651 1. Bhatt S, Gething PW, Brady OJ, Messina JP, Farlow AW, Moyes CL, Drake JM,  
652 Brownstein JS, Hoen AG, Sankoh O, Myers MF, George DB, Jaenisch T, Wint  
653 GR, Simmons CP, Scott TW, Farrar JJ, Hay SI. 2013. The global distribution and  
654 burden of dengue. *Nature* 496:504-7.
- 655 2. Villar L, Dayan GH, Arredondo-Garcia JL, Rivera DM, Cunha R, Deseda C,  
656 Reynales H, Costa MS, Morales-Ramirez JO, Carrasquilla G, Rey LC, Dietze R,  
657 Luz K, Rivas E, Miranda Montoya MC, Cortes Supelano M, Zambrano B,  
658 Langevin E, Boaz M, Tornieporth N, Saville M, Noriega F, Group CYDS. 2015.  
659 Efficacy of a tetravalent dengue vaccine in children in Latin America. *N Engl J*  
660 *Med* 372:113-23.
- 661 3. Screaton G, Mongkolsapaya J, Yacoub S, Roberts C. 2015. New insights into the  
662 immunopathology and control of dengue virus infection. *Nat Rev Immunol*  
663 15:745-59.
- 664 4. Marceau CD, Puschnik AS, Majzoub K, Ooi YS, Brewer SM, Fuchs G,  
665 Swaminathan K, Mata MA, Elias JE, Sarnow P, Carette JE. 2016. Genetic

- 666 dissection of Flaviviridae host factors through genome-scale CRISPR screens.  
667 Nature 535:159-63.
- 668 5. Savidis G, McDougall WM, Meraner P, Perreira JM, Portmann JM, Trincucci G,  
669 John SP, Aker AM, Renzette N, Robbins DR, Guo Z, Green S, Kowalik TF, Brass  
670 AL. 2016. Identification of Zika Virus and Dengue Virus Dependency Factors  
671 using Functional Genomics. Cell Rep 16:232-46.
- 672 6. Cherepanova N, Shrimal S, Gilmore R. 2016. N-linked glycosylation and  
673 homeostasis of the endoplasmic reticulum. Curr Opin Cell Biol 41:57-65.
- 674 7. Ruiz-Canada C, Kelleher DJ, Gilmore R. 2009. Cotranslational and  
675 posttranslational N-glycosylation of polypeptides by distinct mammalian OST  
676 isoforms. Cell 136:272-83.
- 677 8. Cherepanova NA, Shrimal S, Gilmore R. 2014. Oxidoreductase activity is  
678 necessary for N-glycosylation of cysteine-proximal acceptor sites in glycoproteins.  
679 J Cell Biol 206:525-39.
- 680 9. Mohorko E, Owen RL, Malojcic G, Brozzo MS, Aebi M, Glockshuber R. 2014.  
681 Structural basis of substrate specificity of human oligosaccharyl transferase  
682 subunit N33/Tusc3 and its role in regulating protein N-glycosylation. Structure  
683 22:590-601.
- 684 10. Yan Q, Lennarz WJ. 2002. Studies on the function of oligosaccharyl transferase  
685 subunits. Stt3p is directly involved in the glycosylation process. J Biol Chem  
686 277:47692-700.
- 687 11. Walker KW, Lyles MM, Gilbert HF. 1996. Catalysis of oxidative protein folding by  
688 mutants of protein disulfide isomerase with a single active-site cysteine.  
689 Biochemistry 35:1972-80.
- 690 12. Laboissiere MC, Sturley SL, Raines RT. 1995. The essential function of protein-  
691 disulfide isomerase is to unscramble non-native disulfide bonds. J Biol Chem  
692 270:28006-9.
- 693 13. Zhou H, Clapham DE. 2009. Mammalian MagT1 and TUSC3 are required for  
694 cellular magnesium uptake and vertebrate embryonic development. Proc Natl  
695 Acad Sci U S A 106:15750-5.
- 696 14. Watterson D, Modhiran N, Young PR. 2016. The many faces of the flavivirus  
697 NS1 protein offer a multitude of options for inhibitor design. Antiviral Res 130:7-  
698 18.
- 699 15. Naik NG, Wu HN. 2015. Mutation of Putative N-Glycosylation Sites on Dengue  
700 Virus NS4B Decreases RNA Replication. J Virol 89:6746-60.
- 701 16. Lam SS, Martell JD, Kamer KJ, Deerinck TJ, Ellisman MH, Mootha VK, Ting AY.  
702 2015. Directed evolution of APEX2 for electron microscopy and proximity labeling.  
703 Nat Methods 12:51-4.
- 704 17. Houzet L, Jeang KT. 2011. Genome-wide screening using RNA interference to  
705 study host factors in viral replication and pathogenesis. Exp Biol Med (Maywood)  
706 236:962-7.
- 707 18. Roboti P, High S. 2012. The oligosaccharyltransferase subunits OST48, DAD1  
708 and KCP2 function as ubiquitous and selective modulators of mammalian N-  
709 glycosylation. J Cell Sci 125:3474-84.

- 710 19. Cherepanova NA, Gilmore R. 2016. Mammalian cells lacking either the  
711 cotranslational or posttranslocational oligosaccharyltransferase complex display  
712 substrate-dependent defects in asparagine linked glycosylation. *Sci Rep* 6:20946.
- 713 20. Satoh T, Ohba A, Liu Z, Inagaki T, Satoh AK. 2015. dPob/EMC is essential for  
714 biosynthesis of rhodopsin and other multi-pass membrane proteins in *Drosophila*  
715 photoreceptors. *Elife* 4.
- 716 21. Bagchi P, Inoue T, Tsai B. 2016. EMC1-dependent stabilization drives  
717 membrane penetration of a partially destabilized non-enveloped virus. *Elife* 5.
- 718 22. Hatahet F, Ruddock LW. 2007. Substrate recognition by the protein disulfide  
719 isomerases. *FEBS J* 274:5223-34.
- 720 23. Hwang J, Ribbens D, Raychaudhuri S, Cairns L, Gu H, Frost A, Urban S,  
721 Espenshade PJ. 2016. A Golgi rhomboid protease Rbd2 recruits Cdc48 to cleave  
722 yeast SREBP. *EMBO J* 35:2332-2349.
- 723 24. Sanjana NE, Shalem O, Zhang F. 2014. Improved vectors and genome-wide  
724 libraries for CRISPR screening. *Nat Methods* 11:783-4.
- 725 25. Li W, Xu H, Xiao T, Cong L, Love MI, Zhang F, Irizarry RA, Liu JS, Brown M, Liu  
726 XS. 2014. MAGeCK enables robust identification of essential genes from  
727 genome-scale CRISPR/Cas9 knockout screens. *Genome Biol* 15:554.
- 728 26. Bocchinfuso WP, Ma KL, Lee WM, Warmels-Rodenhiser S, Hammond GL. 1992.  
729 Selective removal of glycosylation sites from sex hormone-binding globulin by  
730 site-directed mutagenesis. *Endocrinology* 131:2331-6.
- 731 27. Shrimal S, Gilmore R. 2015. Reduced expression of the  
732 oligosaccharyltransferase exacerbates protein hypoglycosylation in cells lacking  
733 the fully assembled oligosaccharide donor. *Glycobiology* 25:774-83.
- 734 28. Huang CY, Butrapet S, Moss KJ, Childers T, Erb SM, Calvert AE, Silengo SJ,  
735 Kinney RM, Blair CD, Roehrig JT. 2010. The dengue virus type 2 envelope  
736 protein fusion peptide is essential for membrane fusion. *Virology* 396:305-15.
- 737 29. Salloum S, Wang H, Ferguson C, Parton RG, Tai AW. 2013. Rab18 binds to  
738 hepatitis C virus NS5A and promotes interaction between sites of viral replication  
739 and lipid droplets. *PLoS Pathog* 9:e1003513.
- 740 30. Heaton NS, Perera R, Berger KL, Khadka S, Lacount DJ, Kuhn RJ, Randall G.  
741 2010. Dengue virus nonstructural protein 3 redistributes fatty acid synthase to  
742 sites of viral replication and increases cellular fatty acid synthesis. *Proc Natl*  
743 *Acad Sci U S A* 107:17345-50.
- 744 31. Frolova EI, Fayzulin RZ, Cook SH, Griffin DE, Rice CM, Frolov I. 2002. Roles of  
745 nonstructural protein nsP2 and Alpha/Beta interferons in determining the  
746 outcome of Sindbis virus infection. *J Virol* 76:11254-64.
- 747 32. Yi Z, Sperzel L, Nurnberger C, Bredenbeek PJ, Lubick KJ, Best SM, Stoyanov  
748 CT, Law LM, Yuan Z, Rice CM, MacDonald MR. 2011. Identification and  
749 characterization of the host protein DNAJC14 as a broadly active flavivirus  
750 replication modulator. *PLoS Pathog* 7:e1001255.
- 751 33. McGee CE, Shustov AV, Tsetsarkin K, Frolov IV, Mason PW, Vanlandingham DL,  
752 Higgs S. 2010. Infection, dissemination, and transmission of a West Nile virus  
753 green fluorescent protein infectious clone by *Culex pipiens quinquefasciatus*  
754 mosquitoes. *Vector Borne Zoonotic Dis* 10:267-74.

- 755 34. Tsetsarkin K, Higgs S, McGee CE, De Lamballerie X, Charrel RN,  
756 Vanlandingham DL. 2006. Infectious clones of Chikungunya virus (La Reunion  
757 isolate) for vector competence studies. *Vector Borne Zoonotic Dis* 6:325-37.
- 758 35. Atasheva S, Krendelchtchikova V, Liopo A, Frolova E, Frolov I. 2010. Interplay of  
759 acute and persistent infections caused by Venezuelan equine encephalitis virus  
760 encoding mutated capsid protein. *J Virol* 84:10004-15.
- 761 36. Schoggins JW, Dorner M, Feulner M, Imanaka N, Murphy MY, Ploss A, Rice CM.  
762 2012. Dengue reporter viruses reveal viral dynamics in interferon receptor-  
763 deficient mice and sensitivity to interferon effectors in vitro. *Proc Natl Acad Sci U*  
764 *S A* 109:14610-5.
- 765 37. Lanciotti RS, Lambert AJ, Holodniy M, Saavedra S, Signor Ldel C. 2016.  
766 Phylogeny of Zika Virus in Western Hemisphere, 2015. *Emerg Infect Dis* 22:933-  
767 5.
- 768 38. Hung V, Udeshi ND, Lam SS, Loh KH, Cox KJ, Pedram K, Carr SA, Ting AY.  
769 2016. Spatially resolved proteomic mapping in living cells with the engineered  
770 peroxidase APEX2. *Nat Protoc* 11:456-75.
- 771 39. Wang H, Perry JW, Lauring AS, Neddermann P, De Francesco R, Tai AW. 2014.  
772 Oxysterol-binding protein is a phosphatidylinositol 4-kinase effector required for  
773 HCV replication membrane integrity and cholesterol trafficking. *Gastroenterology*  
774 146:1373-85 e1-11.
- 775

776



777 **Figure legends**

778

779 **Figure 1**

780 **The CRISPR-Cas9 screen reveals the oligosaccharyltransferase complex as**

781 **essential to DENV propagation. A**, Depiction of the whole-genome CRISPR screen

782 selecting for knockout cells resistant to dengue virus infection. **B**, Diagram of the two

783 OST complexes that contain either STT3A or STT3B. Subunits of the OST complex

784 shaded in blue were significantly enriched in the screen. **C**, Table of the hits from the

785 screen showing the gene ID, p-value, and false discovery rate as calculated by

786 MaGECK analysis.

787

788 **Figure 2**

789 **The catalytic activities of STT3A or STT3B are not required for DENV replication.**

790 **A**, Huh 7.5.1 cells were transduced with a lentivirus encoding a puromycin resistance

791 marker, Cas9, and a single guide RNA (sgRNA) targeting the indicated genes. The

792 sgRNAs targeting GFP act as a negative control. Cells were infected with luc-DENV for

793 3 d and luciferase activity was measured in relative light units (RLU). Below, Western

794 blots for the indicated proteins are shown. Arrows indicate non-specific bands. **B and C**,

795 knockout cells were transduced with lentiviral vectors to rescue expression of the

796 indicated protein. “STT3A dead” is a catalytically inactive W526A/D527A double mutant.

797 “STT3B dead” is a catalytically inactive W605A/D606A double mutant with a C-terminal

798 V5 tag. Transient transfection of constructs to express pSAP and SHBG were used to

799 assess STT3A and STT3B catalytic activity. Below, Western blots show the expression

800 of the indicated proteins. **D**, knockout cells were transiently transfected with a luc-DENV  
801 replicon and luciferase activity was measured 72 h post-transfection (hpt). Data is  
802 plotted as a ratio of 72 hpt / 4 hpt to control for transfection efficiency. GDD indicates a  
803 polymerase dead replicon with replacement of the GNN active site sequence in the NS5  
804 RNA polymerase by GDD. For A-D, data are expressed as means with SD for three  
805 independent biological replicates. Statistical significance was determined by Student's t-  
806 test, where \* $p < 0.05$ , \*\* $p < 0.005$ , and \*\*\* $p < 0.0005$ . In A, means were compared to GFP  
807 sgRNA #2. In B and C, means were compared to their respective knockouts. In D,  
808 means were compared to the GFP control.

809

### 810 **Figure 3**

#### 811 **The oxidoreductase activity of MAGT1 is required for DENV replication.**

812 **A**, CRISPR modified Huh 7.5.1 MAGT1 knockout cells were transduced to express  
813 MAGT1 or TUSC3-HA. The AxxA MAGT1 and TUSC3-HA mutants were generated by  
814 mutating CxxC active sites to AxxA. Below, Western blots for the indicated proteins are  
815 shown. The MAGT1 antibody cross-reacts weakly with TUSC3. **B**, MAGT1 knockout  
816 cells were transduced to express MAGT1 mutants with the indicated mutations. Below,  
817 Western blots for the indicated proteins are shown. For A and B, cells were infected with  
818 luc-DENV and luciferase activity was measured at 3 days post-infection. Data are  
819 expressed as means with SD for three independent infections. Statistical significance  
820 was determined by Student's t-test, where \* $p < 0.05$ , \*\* $p < 0.005$ , and \*\*\* $p < 0.0005$ . In A  
821 and B, means were compared to MAGT1 knockout cells without any additions. **C**,  
822 immunofluorescence shows the localization of MAGT1 in uninfected cells or two days

823 post-infection with DENV. MAGT1 knockout cells were transduced to express HA  
824 tagged MAGT1 (WT or AxxA), as indicated on the left. Cells were fixed, permeabilized,  
825 and stained with antibodies to the indicated proteins.

826

## 827 **Figure 4**

### 828 **Glycosylation of NS4B is mediated by STT3B**

829 **A**, Huh 7.5.1 cells ablated for the indicated genes were transfected to express NS4B-V5  
830 (lanes 1-6) or were mock transfected (lanes 7-12). Lysates were then subjected to  
831 PNGase F treatment to remove N-linked glycans from proteins, which were then  
832 resolved by SDS-PAGE and visualized by Western blotting for the indicated proteins. **B**,  
833 STT3B knockout 293T cells were stably transduced to express either STT3B wild-type  
834 or catalytically inactive “STT3B-dead”. These cells were then transfected to express  
835 NS4B-HA, and lysates were subjected to SDS-PAGE and Western blot. In A and B, the  
836 black arrows indicate nonspecific background bands, and asterisks (\*) mark the NS4B  
837 specific PNGase F sensitive bands.

838

## 839 **Figure 5**

### 840 **MAGT1 is in close proximity to NS4B and NS1 during DENV infection**

841 Cells stably transduced to express APEX2-MAGT1 were infected with DENV-2 or mock  
842 infected for 2 days. In all conditions, biotin-phenol was added to the cell media for 30  
843 min. Where indicated, APEX2 was activated with hydrogen peroxide for 1 min to  
844 biotinylate APEX2-MAGT1 proximal proteins prior to quenching and lysis. The far right  
845 lane is a negative control where APEX2 was not activated. Biotinylated proteins were

846 immunoprecipitated with streptavidin beads, and lysates were resolved by SDS-PAGE.  
847 Western blotting was performed for the indicated proteins for both the IP samples and  
848 the input.

849

## 850 **Supplemental Figures**

### 851 **S1. Viability of OST knockout cells**

852 Huh 7.5.1 cells were transduced with lentiviral vectors coexpressing Cas9 with sgRNAs  
853 targeting the indicated genes. Cell viability was measured by Cell-Titer Glo over the  
854 course of 4 days for 3 independent wells. Data is plotted relative to day 1 to normalize  
855 for differences in number of cells initially plated. P indicates the parental Huh7.5.1 cells.

856

### 857 **S2. Inhibition of flavivirus infection in OST knockout cells.**

858 Huh 7.5.1 cells were transduced to express two independent sgRNAs targeting STT3A,  
859 STT3B, or one sgRNA targeting GFP as a control. Cells were then infected with the  
860 indicated fluorescent protein-expressing reporter viruses (See Materials and Methods  
861 for detailed description of the viruses) and subjected to flow cytometry to measure the  
862 number of infected cells. ZIKV infection was detected by immunostaining followed by  
863 flow cytometry. Data are plotted as a percentage relative to control cells expressing an  
864 sgRNA targeting GFP for three independent infections. Statistical significance was  
865 determined by Student's t-test, where means were compared to GFP control, and  
866 \* $p < 0.05$ , \*\* $p < 0.005$ , and \*\*\* $p < 0.0005$ .

867

### 868 **S3. Catalytic mutants of MAGT1 associate with STT3B.**

869 293T cells expressing the indicated mutants of MAGT1-HA were transfected to express  
870 STT3B-V5. The terms 87 and 90 refer to the C87A and C90A mutants, respectively.  
871 Cells were lysed and co-immunoprecipitation was carried out using an anti-HA antibody.  
872 Shown are Western blots detecting the specified proteins. Mutants of MAGT1 migrate  
873 as two distinct bands.

874

875 **S4. NS1 glycosylation and dimerization are unchanged in the absence of STT3A,**  
876 **STT3B, or MAGT1**

877 **A**, the indicated CRISPR knockout 293T cells were transfected to express NS1-FLAG.  
878 Lysates were treated with PNGase F to remove N-linked glycans followed by Western  
879 blotting to visualize differences in migration of NS1. The glycosylated and de-  
880 glycosylated forms of NS1 are indicated. **B**, A 5 min pulse with <sup>35</sup>S-cysteine/methionine  
881 was followed by a 20 min chase to visualize differences in the efficiency of NS1  
882 glycosylation and dimerization in CRISPR-edited HEK293 cells. Endoglycosidase H  
883 treatment was used to indicate the mobility of unglycosylated NS1 by SDS-PAGE.

884

885 **S5. NS1-NS2A processing is unaffected by the loss of STT3B.**

886 Wild-type 293T cells or 293T cells transduced to express an sgRNA targeting STT3B  
887 were transfected to express NS1-NS2A-V5. Cell lysates were resolved by SDS-PAGE  
888 and visualized by Western blot using an anti-V5 antibody to probe for processed and  
889 unprocessed NS2A.

890

891 **S6. The redox status of NS4B is unchanged in the absence of MAGT1.**

892 The indicated CRISPR knockout 293T cells were transfected to express pNS4B-HA. We  
893 used STT3B knockout cells to deplete both MAGT1 and TUSC3. Cells were lysed in  
894 buffer with the specified additions of NEM, mPEG, or TCEP. Western blots were carried  
895 out to determine the migration patterns of NS1 and NS4B in the given conditions. The  
896 number of estimated maleimide-PEG modifications is indicated on the right.

897

### 898 **S7. A potential model for disulfide isomerization by single-cysteine MAGT1**

899 A MAGT1 mutant containing a single cysteine active site (AxxC or CxxA) is shown in  
900 yellow. In blue is a target protein, such as NS4B, which contains multiple cysteines that  
901 may form disulfide bonds. This protein has a non-native disulfide arrangement that is  
902 identified by MAGT1. Through its active site cysteine, MAGT1 forms a mixed disulfide  
903 with the target protein, reducing the incorrect disulfide bond. The correct disulfide bond  
904 is then formed by a cysteine from the target protein, resolving the mixed disulfide  
905 between MAGT1 and its target.

906

### 907 **Table S1. Comparison of hits from the screen**

908 A list of the top 25 significant hits from biological replicates were compared to hits from  
909 two previously published screens. Gene names are colored to indicate groups of ER  
910 complexes. Yellow indicates genes encoding components of the EMC complex, blue  
911 indicates components of the OST complexes, and green indicates components of the  
912 ER associated degradation pathway (ERAD). The rank of each hit in independent  
913 biological replicates is shown in the second and third columns. The false discovery rate  
914 calculated by MAGECK and the number of sgRNAs classified as a hit by MaGECK in

915 our screen are shown. Hits from our screen that were also identified in the top 25 hits of  
916 Marceau *et al.* or the top 150 of Savidis *et al.* are marked with an X.

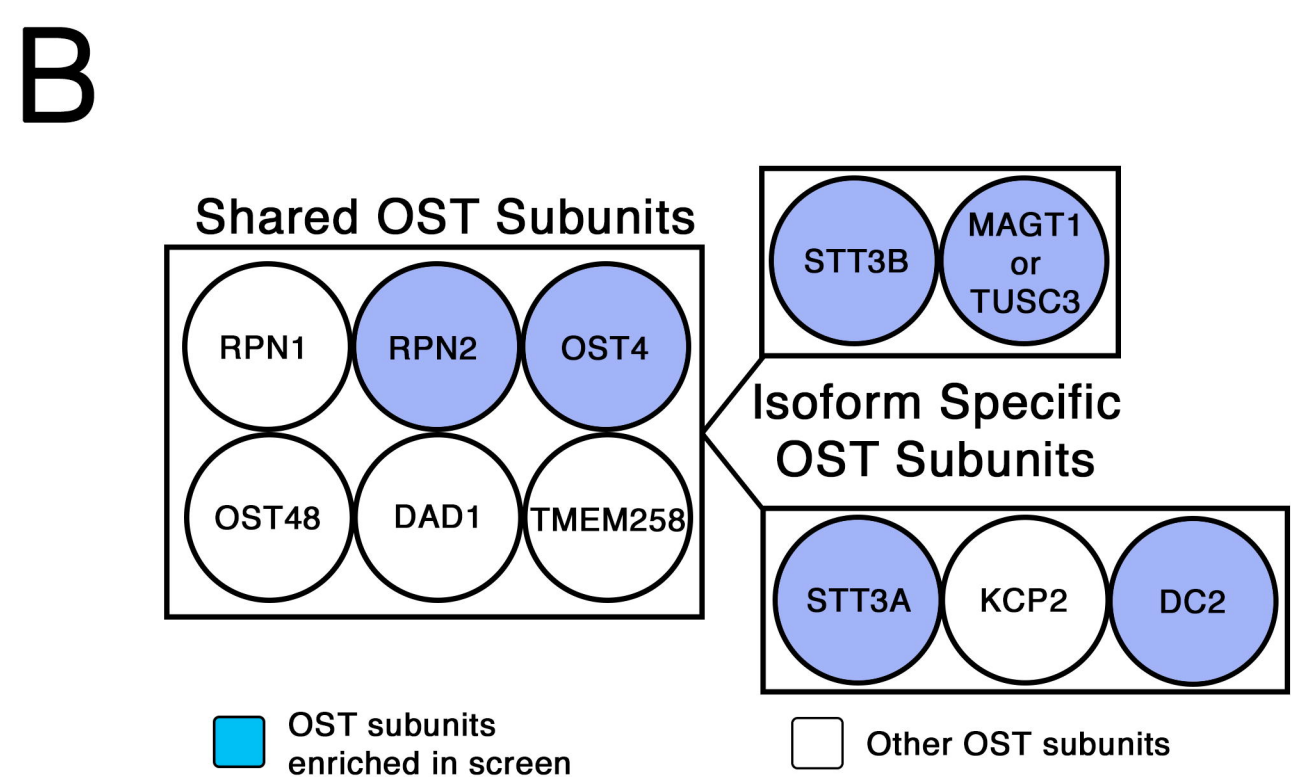
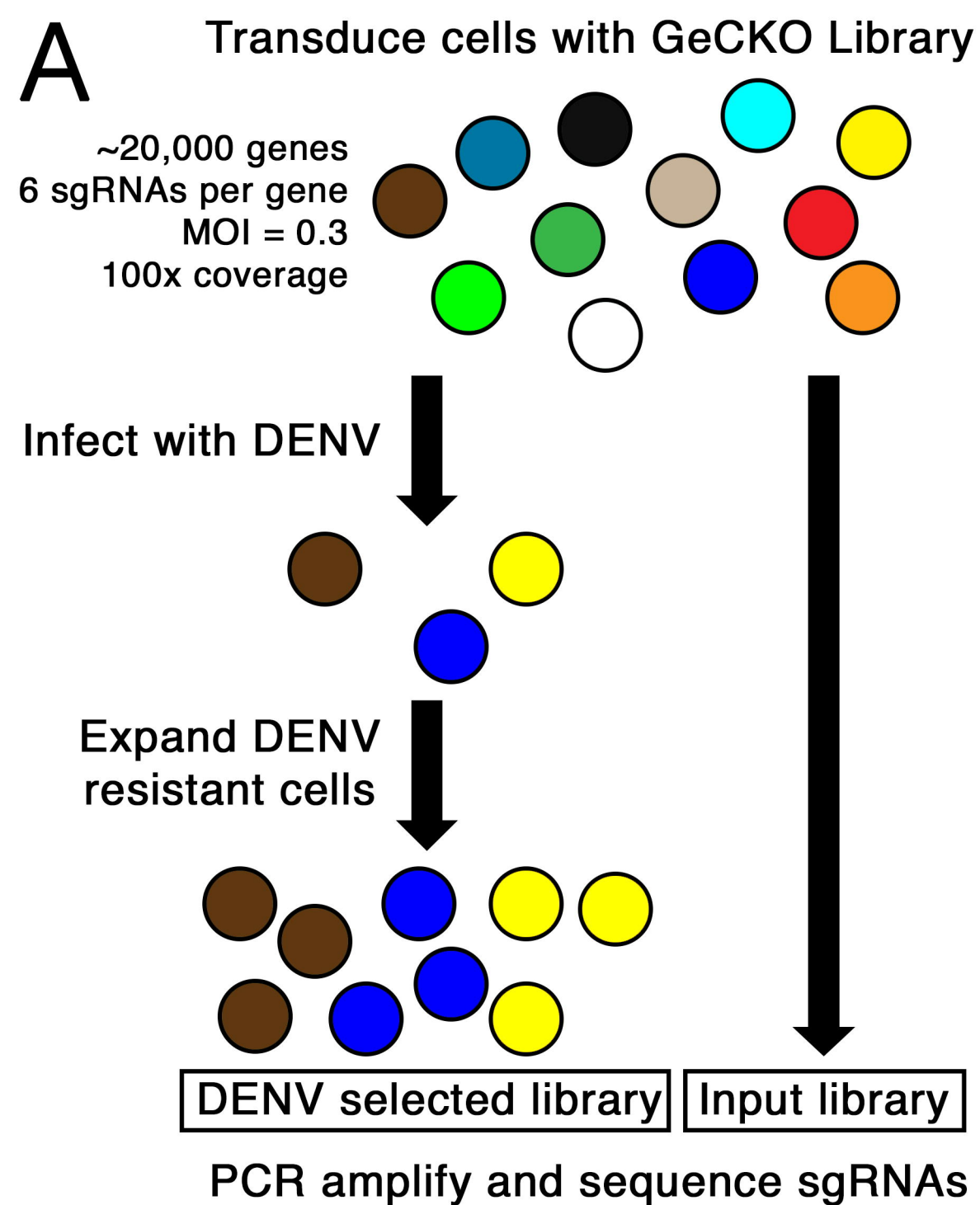
917

918 **Table S2. List of crRNAs used to generate knockout cells**

919 Oligonucleotides were cloned into pLENTICRISPRv2 to generate lentiviruses for

920 CRISPR mediated knockout of specific OST genes.

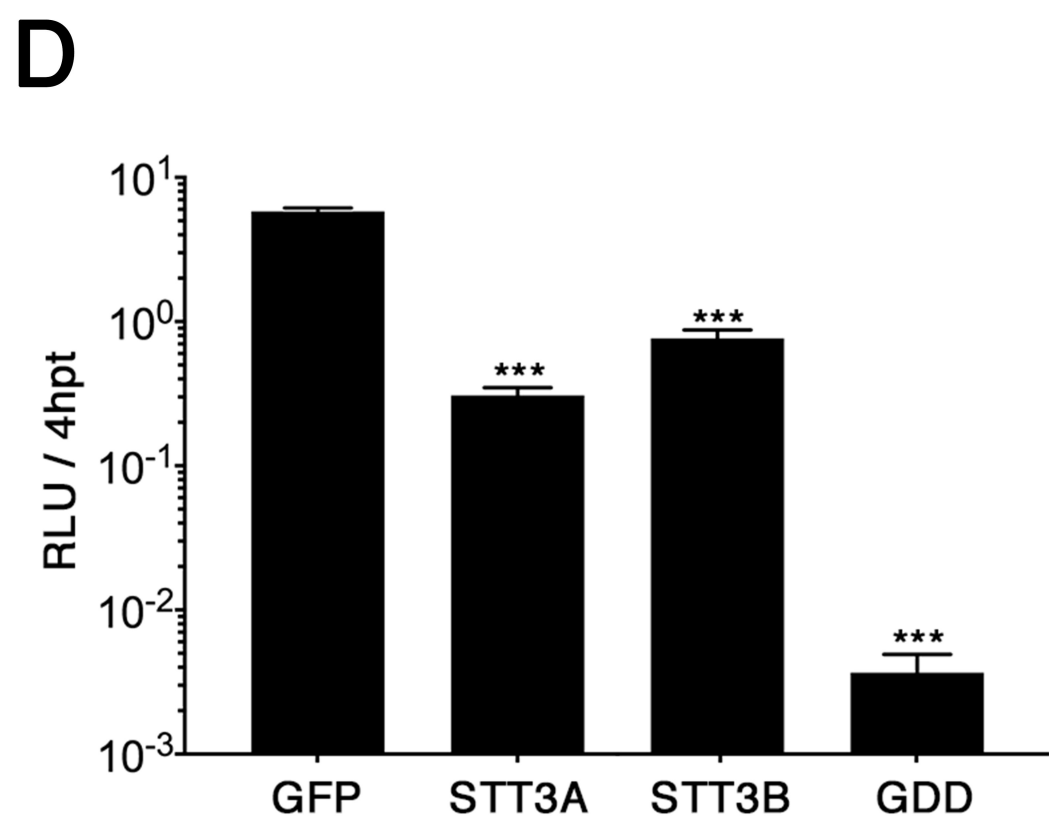
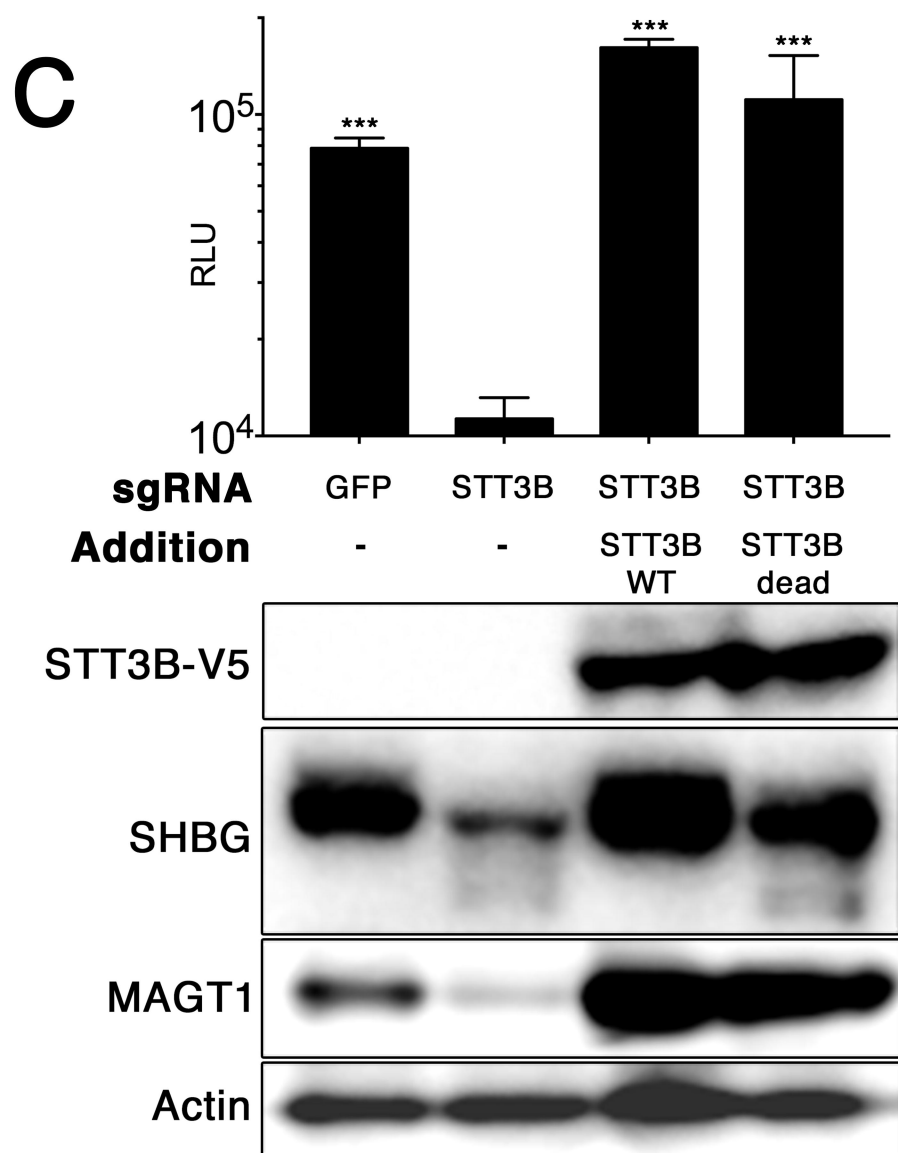
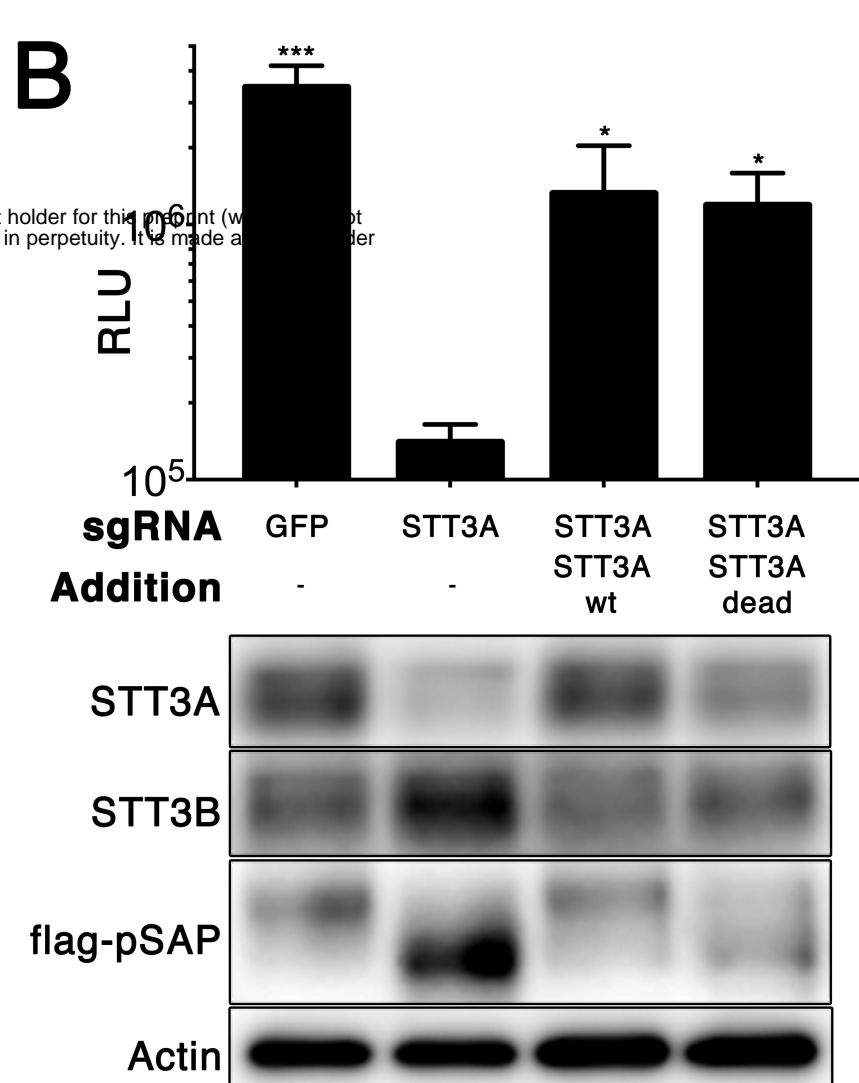
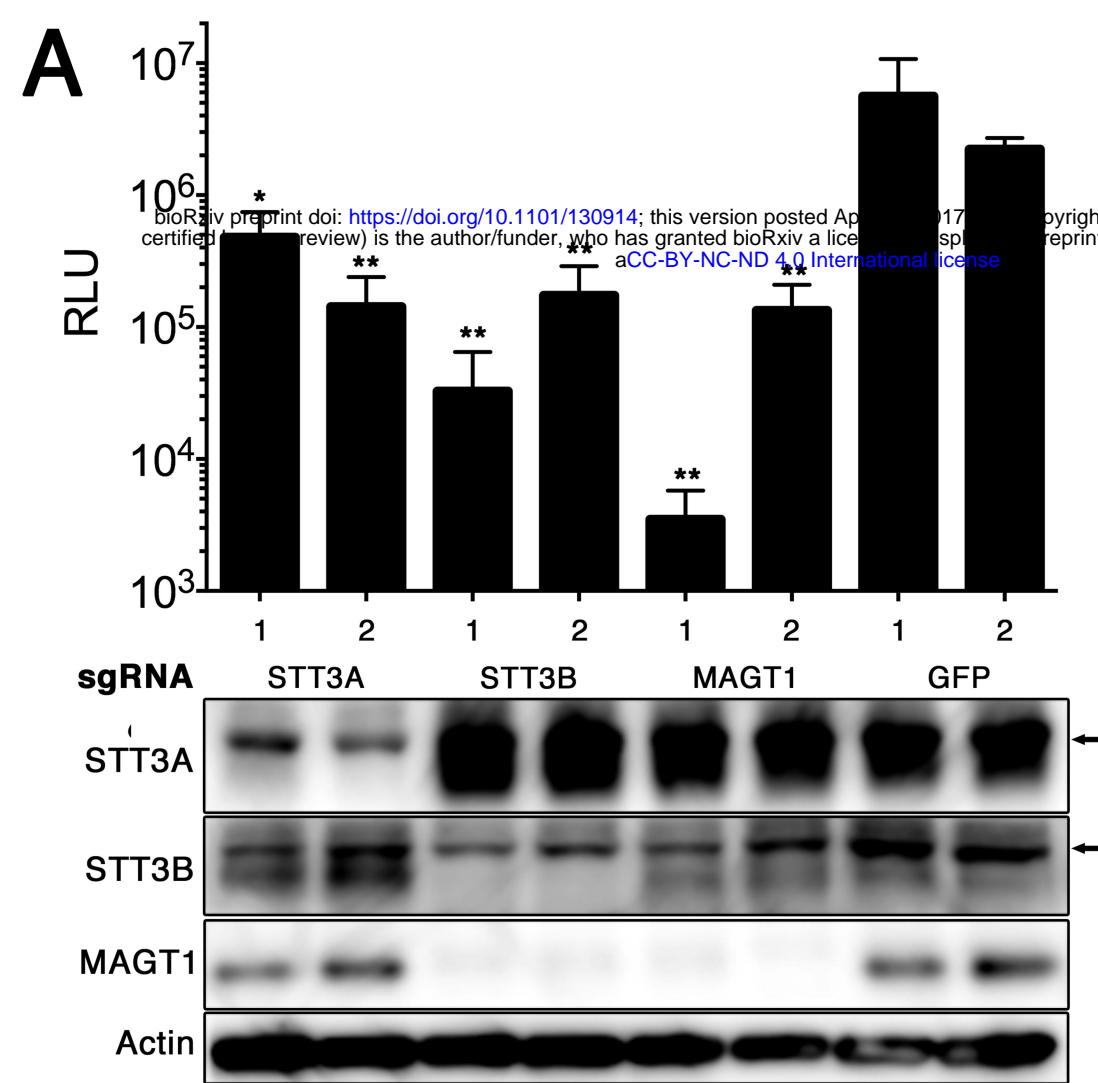
921

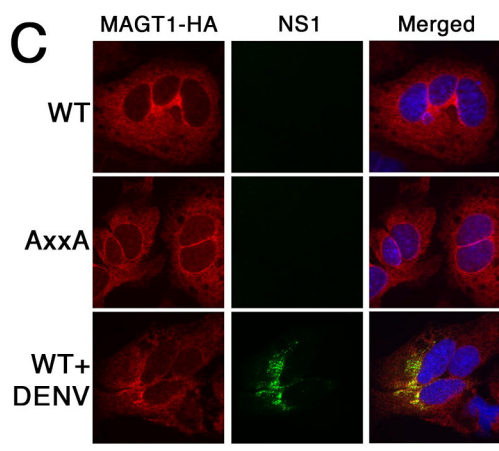
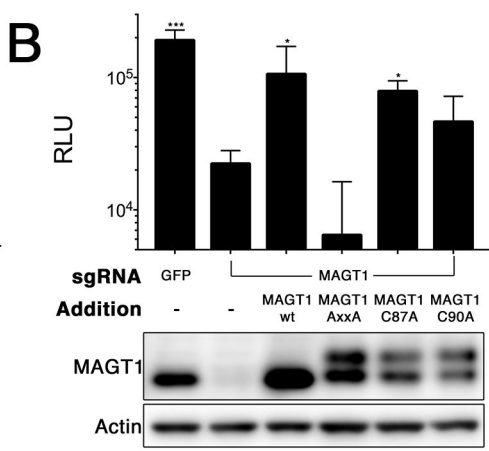
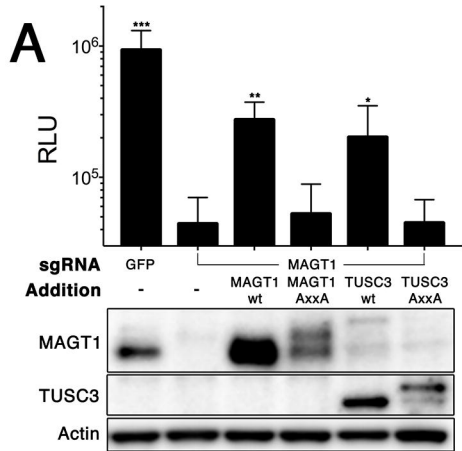


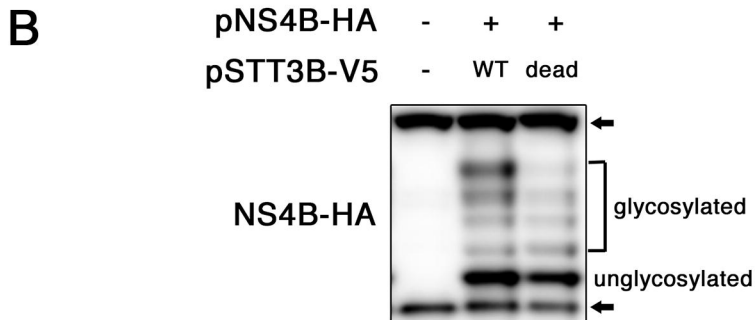
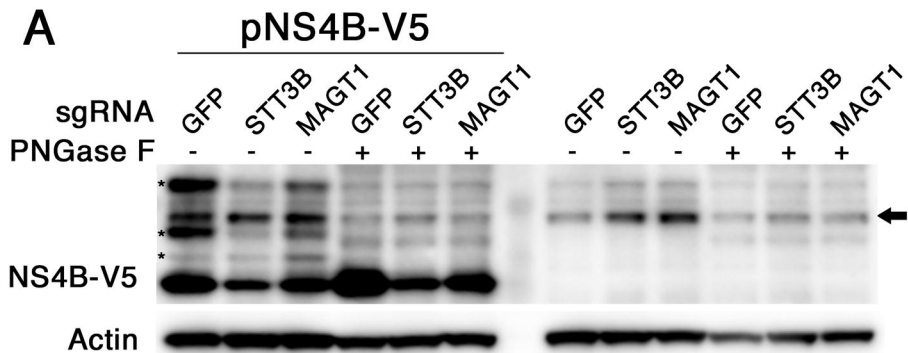
**C**

	P-value	False Discovery Rate	Enriched sgRNAs
STT3A	2.22E-07	0.00045	6
MAGT1	2.22E-07	0.00045	6
STT3B	2.22E-07	0.00045	5
RPN2	2.22E-07	0.00045	5
OST4	4.73E-05	0.058581	3
DC2	0.0013308	0.570164	3









DENV-2	+	-	+
BP	+	+	+
H <sub>2</sub> O <sub>2</sub>	+	+	-

